Power System Dynamic State Estimation With Synchronized Phasor Measurements

Farrokh Aminifar, *Member, IEEE*, Mohammad Shahidehpour, *Fellow, IEEE*, Mahmud Fotuhi-Firuzabad, *Senior Member, IEEE*, and Saeed Kamalinia, *Member, IEEE*

***Abstract*— The dynamic state estimation (DSE) applied to power systems with synchrophasor measurements would estimate the system's true state based on measurements and predictions. In this application, as phasor measurement units (PMUs) are not deployed at all power system buses, state predictions would enhance the redundancy of DSE input data. The significance of predicted and measured data in DSE is affected by their confidence levels, which are inversely proportional to the corresponding variances. In practice, power system states may undergo drastic changes during hourly load fluctuations, component outages, or network switchings. In such conditions, the inclusion of predicted values could degrade the power system state estimation. This paper presents a mixed-integer programming formulation of DSE that is capable of simultaneously discarding predicted values whenever sudden changes in the system state are detected. This feature enhances the DSE computation and will not require iterative executions. The proposed model accommodates system-wide synchronized measurements of PMUs, which could be of interest to smart grid applications in energy management systems. The voltage phasors at buses without PMUs are calculated via voltage and current measurements of adjacent buses, which are referred to as indirect measurements. The guide to the expression of uncertainty in measurement is used for computing the confidence level of indirect measurements based on uncertainties associated with PMU measurements as well as with transmission line parameters. Simulation studies are conducted on an illustrative three-bus example and the IEEE 57-bus power system, and the performance of the proposed model is thoroughly discussed.**

***Index Terms*— Dynamic state estimation, mathematical programming, power system monitoring, state prediction, synchrophasor measurement, uncertainty propagation.**

NOMENCLATURE

Indexes

b	Bus index.
i	State variable index.
j	Measurement index.
l	Line index.
p	Uncertain parameter index.
t	Time period index.

Sets

P	Set of uncertain parameters.

Parameters

$I_l \angle \delta_{I_l}$	Current phasor of line l.
M_i	Large positive constant associated with state variable i.
NB	Number of buses.
NM_i	Number of measurements associated with state variable i.
NS	Number of states.
NT	Number of time periods.
$r_i^{\max}, r_i^{\min}$	Upper and lower limits of $\tilde{r}_{it}$.
$V_b \angle \delta_b$	Voltage phasor of bus b.
Y, θ_y, G, B	Line admittance parameters.
Z, θ_z, R, X	Line impedance parameters.
α_i, β_i	Parameters of the prediction model associated with state variable i.
$\bar{\sigma}_{ij}$	Standard deviation of measurement j associated with state variable i.
σ_p	Standard deviation of parameter p.

Variables

D_{it}, C_{it}	Coefficients of the prediction model associated with state variable i at period t.
J_t	Objective function value at period t.
$\tilde{r}_{it}$	Residual of prediction associated with state variable i at period t.
$\bar{r}_{ijt}$	Residual of measurement j associated with state variable i at period t.
w_{it}, σ_{it}	Fluctuation and its standard deviation associated with state variable i at period t.
x_{it}	True value of state variable i at period t.
$\bar{x}_{ijt}$	Measurement j associated with the state variable i at period t.
$\tilde{x}_{it}, \tilde{\sigma}_{it}$	Prediction and its standard deviation associated with state variable i at period t.
$\hat{x}_{it}, \hat{\sigma}_{it}$	Estimation and its standard deviation associated with the state variable i at period t.
γ_{it}	Binary variable to discard the prediction associated with state variable i at period t.
RMSD	Sate estimator performance index.

Manuscript received August 12, 2012; revised June 2, 2013; accepted June 3, 2013. The Associate Editor coordinating the review process was Dr. Carlo Muscas.

F. Aminifar is with the School of Electrical and Computer Engineering, College of Engineering, the University of Tehran, Tehran 14174, Iran (e-mail: aminifar@ece.ut.ac.ir).

M. Shahidehpour is with the Galvin Center for Electricity Innovation, the Illinois Institute of Technology, Chicago, IL 60616 USA (e-mail: ms@iit.edu).

M. Fotuhi-Firuzabad is with the Center of Excellence in Power system Control and Management, Electrical Engineering Department, Sharif University of Technology, Tehran 145888, Iran (e-mail: fotuhi@sharif.edu).

S. Kamalinia is with the Power System Solutions Division of S&C Electric Company, Chicago, IL 60626 USA (e-mail: saeed.kamalinia@sandc.com).

Color versions of one or more of the figures in this paper are available online at http://ieeexplore.ieee.org.

Digital Object Identifier 10.1109/TIM.2013.2278595

I. Introduction

STATE estimation (SE) computes the best estimate of the true operating state of a power system as a prerequisite for an efficient and reliable operation [1]. Since SE serves several crucial functions such as the detection of abnormal conditions, generator correction actions, and contingency analysis [2], its responsibility is increasing with the dimension of power systems and emerging uncertain conditions in the operation of restructured systems.

In general, SE is categorized into the following three classes: 1) static SE (SSE); 2) tracking SE (TSE); and 3) dynamic SE (DSE) [3]. SSE estimates the power system state associated with a given time and based on the measurement set corresponding to that moment of time. The SSE algorithm is iterative that is initialized as a flat start. Hence, it uses heavy computations and cannot be executed in short intervals. To mitigate this burden, TSE was introduced in which the estimation starts from the last calculated state variables instead of a flat point. In both SSE and TSE, the power system state is estimated based on a single set of measurements. A more advanced class of estimators is DSE, also referred to as forecasted-aided SE, which is becoming more practical in modern energy management systems. DSE possesses the ability to predict the power system state progressively in short time steps. Furthermore, at each time step, the estimation uses both measurement and prediction data sets. A comprehensive survey of DSE techniques and models along with the results of DSE implementation in practical power systems have been presented in [4] and [5]. Other reviews of DSE techniques are available in [6] and [7]. One of the challenging aspects of applying DSE is the estimation error arising from the utilization of historical-based prediction data during drastic changes in the power system state variables.

A new generation of power system monitoring schemes embedded in the wide-area measurement system (WAMS) is enabled by escalating the deployment of phasor measurement units (PMUs) [8]. PMUs directly measure the state variables, i.e., magnitude and phase angle of bus voltages, with a very high accuracy. They can consequently increase the robustness and precision of the estimation process. The superiorities of WAMS over the conventional metering infrastructure are as follows [9].

1) PMUs are installed with specific guidelines, tested during the commissioning process, and calibrated periodically.
2) PMU devices are furnished with advanced computation algorithms and self-check/self-diagnostic capabilities. In addition, PMUs are equipped with 16 bit or upper A/D converters providing an extra high sampling rate and very accurate measurements.
3) GPS receiver is added to the PMU structure for synchronizing the A/D phase locked loop (sampling clock) and accompanying the PMU data with the exact time of measurement. The quality of time synchronization associated with the data is sent as well.
4) PMUs report measurements to phasor data concentrator at the rate of 50/60 samples/s for 50/60 Hz systems.
5) Similar to digital fault recorders, PMU devices are usually responsible for recording sinusoidal signals which are downloadable through the direct access to PMUs.

The incorporation of PMU measurements in the conventional DSE was discussed in [10]–[15]. In addition, the Electric Power Research Institute had a research project relevant to this issue [16]. To avoid deficits associated with the conventional metering system such as asynchronous measurement and time skew errors, a plenary set of WAMS is intended in future power systems [17]. The high reporting rate of PMUs, commissioning high speed communication facilities in substations, and developing fast and efficient DSE algorithms are three key forces for decreasing the time interval of successive estimations. The reduction of time interval would be very desirable for near real-time applications.

The most common DSE algorithms are variants of weighted least squares (WLSs) estimation. These models are solved using iterative matrix-based calculations along with mathematical heuristics to reduce the computation [18]. An alternative way for DSE is mixed-integer programming (MIP) formulation, which can efficiently be solved by commercially available solvers [19].

This paper presents an MIP formulation of DSE that is based on PMU measurements. The proposed method accelerates the DSE execution and is capable of simultaneously discarding predictions from the estimation process when estimated states exceed the estimation confidence bound. In practice, it is neither economical nor essential to equip all buses with PMUs. Hence, the power system state variables would be calculated based on PMU measurements at adjacent buses. The calculated confidence level would be affected by uncertainties associated with PMU measurements. In addition, transmission line parameters are usually assumed to be exact while they are not indeed. The uncertainty of these parameters is considered in this paper for the calculation of PMU indirect measurements. An illustrative example and the IEEE 57-bus test system are examined in this paper for investigating performance of the proposed DSE model.

The rest of this paper is organized as follows. Section II describes the error propagation phenomenon in the calculation of voltage phasors associated with buses not having PMU. A general introduction to DSE is described in Section III. The proposed DSE model and formulation are presented in Section IV. Section V discusses the numerical examples. Concluding remarks are outlined in Section VI. The Appendix presents formulas derived for the calculating error propagation.

II. Standard Deviation of Indirect Measurements

A PMU installed at any bus would measure the corresponding voltage and current phasors. Using the phasors at one end of a transmission line, the corresponding phasors can be calculated at the other end [9]. The DSE algorithm incorporates the confidence level of all measurements either directly measured or indirectly calculated. Accordingly, the

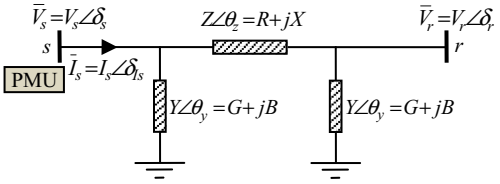

Fig. 1. Phasor measurement and calculation in a transmission line.

confidence in the indirect phasors measurement is required which can be calculated by three approaches including the uncertainty propagation, Monte Carlo simulation, and random fuzzy variables. Fixed transmission line parameters are assumed in [20], which may not be the case in practice. For instance, the line resistance is dependent on the ambient temperature, and the asymmetry of three-phase currents could impact the line reactance. A typical uncertainty bound for line parameters is $\pm 2\%$ [21]. Hence, it is imperative to model line parameter uncertainties, which are discussed in this section.

The inaccuracy of conventional measurement devices for measuring voltage, current, and power quantities, is usually over $\pm 1\%$ of the full scale [18]. In contrast, PMU measurements are much more precise and time tagged with an accuracy of better than 1 μs [9]. They are, however, still prone to precision errors due to the inaccuracy of PMU instruments including transformers, cables, and A/D converters [22]. The first two sets of random errors are mostly biased and can be compensated by sophisticated PMU calibration techniques [23]. The A/D-induced errors are more random and consequently difficult to eliminate. The total vector error (TVE) is a measure of the PMU measurement accuracy level with acceptable ranges in steady-state and dynamic conditions, which are provided in the IEEE C37.118.1 standard [24].

Fig. 1 shows the π model of a transmission line between buses s and r and a PMU located at bus s. The PMU measures the voltage phasor of bus s and the current phasor of the line connected to bus s. Hence

$$V_r \angle \delta_r = V_s \angle \varphi_1 - I_s Z \angle \varphi_2 + V_s Y Z \angle \varphi_3 \tag{1}$$

where $\varphi_1 = \delta_s$, $\varphi_2 = \delta_{Is} + \theta_z$, and $\varphi_3 = \delta_s + \theta_y + \theta_z$. Since

$$P = \{V_s, \delta_s, I_s, \delta_{Is}, Z, \theta_z, Y, \theta_y\} \tag{2}$$

through applying the guide to the expression of uncertainty in measurement (GUM), the standard deviations of V_r and δ_r are calculated as

$$\sigma_{V_r} = \sqrt{\sum_{p \in P} \left[\partial V_r / \partial p\right]^2 \left[\sigma_p\right]^2} \tag{3}$$

$$\sigma_{\delta_r} = \sqrt{\sum_{p \in P} \left[\partial \delta_r / \partial p\right]^2 \left[\sigma_p\right]^2} \tag{4}$$

and the corresponding detailed formulation is presented in the Appendix.

We assume that the random measurement error is represented by a normal distribution. Thus, the standard deviation of each PMU measurement, i.e., V_s, δ_s, I_s, and δ_{Is}, would be one sixth of the corresponding confidence intervals. A uniform distribution function is assumed for the random transmission parameter error in which the standard deviation is $(2\sqrt{3})^{-1}$ of the associated confidence intervals. The calculations in this section correspond to buses without PMU. The PMU placement scheme is assumed to be given by either deterministic or probabilistic studies [25]–[28].

III. Dynamic State Estimation

A. General Background

DSE has two objectives: 1) prediction of power system state at the next time period and 2) SE based on both sets of predicted and measured data. The first feature provides the power system operator an additional time for making control decisions and analyzing the security of operating system. Talking specifically about WAMS, this feature is less important since the measurement time instants are very close. The second attribute would significantly improve the performance of DSE. The consideration of predicted values in the estimation process would enhance the data redundancy and make the DSE more robust as compared with SSE and TSE, which use real measurements alone.

Two consecutive stages are recognized in DSE which are state prediction and SE (it is referred to as state filtering in some documents). The power system state at the next time period is predicted at the first stage, and upon receiving the measurement set, the system state is determined by the estimation process.

B. Major DSE Challenges

Power systems follow a quasi-static regime as the daily load profile is followed by small random fluctuations. This situation is referred to as normal operating condition in which the power system state varies slowly and the performance of DSE is highly satisfactory. The major DSE challenge occurs during sudden changes in power system conditions including abrupt changes in load and generation and network reconfiguration [29]. When a sudden change occurs, state variables that are geographically close to the affected area could experience large transitions. Hence, there could be large differences between actual measurements and predictions based on historical data. In such cases, the predictions could affect the final estimated values and render degradation of the overall performance of DSE. The proposed solutions to this shortcoming are reviewed as follows.

The first proposed approach to detect the sudden change condition is based on the innovation analysis [3]–[5], [29]–[32]. This method compares the predicted measurements with the real measurement set and decides whether or not a sudden change condition has occurred. Two methods are offered to deal with this situation: 1) deemphasizing the importance of predicted values by reducing their weight (or analogously attach a higher weight to the measurements) and 2) labelling the prediction as unreliable and perform SSE or TSE.

An algorithm to increase the robustness of DSE has been proposed in [33] and [34]. In contrast to the approach based on the innovation analysis, this technique does not need

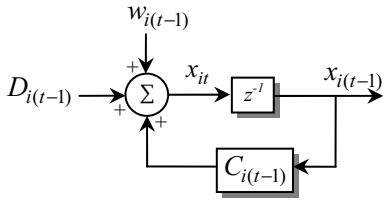

Fig. 2. Dynamic system with linear characteristic.

to detect the anomaly conditions and remedy them at two separate stages. In [33] and [34], it was illustrated that the proposed method, in spite of its effectiveness during bad data and topology error conditions, does not work well in sudden change conditions. The application of fuzzy controllers to intelligently guide the solution to a near-optimal trajectory has been proposed in [35]. This technique calculates the difference between predicted and estimated states. If the difference is greater than a small threshold, a compensation vector is generated and the estimation stage is repeated. Accordingly, the estimation stage of DSE will be longer.

IV. Proposed DSE Formulation and Methodology

For a power system with NB buses, the state vector will have NB bus voltage magnitudes and NB phase angles; hence, the number of state variables, NS, would be the same as 2NB. In the following, the two DSE stages are formulated and discussed.

A. State Prediction

In a linear dynamic power system, shown in Fig. 2, the estimation process is presented as

$$x_{it} = C_{i(t-1)}x_{i(t-1)} + D_{i(t-1)} + w_{i(t-1)} \tag{5}$$

where x_{it} is the system state, $C_{i(t-1)}$ and $D_{i(t-1)}$ are model coefficients, and $w_{i(t-1)}$ is the random change of the power system state. $w_{i(t-1)}$ is a white Gaussian sequence with zero mean and the standard deviation of $\sigma_{i(t-1)}$.

Equation (5) shows that the new power system state could be represented as a function of the past state (s). Accordingly, the next power system state is readily predicted based on the information obtained in $t-1$.

Applying the conditional expectation operator on (5), the power system state at the next time period is obtained as

$$\tilde{x}_{it} = C_{i(t-1)}\hat{x}_{i(t-1)} + D_{i(t-1)} \tag{6}$$

and the variance associated with the prediction would be

$$\tilde{\sigma}^2_{it} = C^2_{i(t-1)}\hat{\sigma}^2_{i(t-1)} + \sigma^2_{i(t-1)}. \tag{7}$$

The coefficients used in (5) are specified according to the adopted prediction method. The commonly used prediction technique in DSE is the Holt's linear exponential smoothing technique [35], which is employed here. The following equations were proposed by [36] for the Holt's method

$$C_{i(t-1)} = \alpha_i(1+\beta_i) \tag{8}$$

$$D_{i(t-1)} = (1+\beta_i)(1-\alpha_i)\tilde{x}_{i(t-1)} - \beta_i S_{i(t-2)} + (1-\beta_i)b_{i(t-2)} \tag{9}$$

$$S_{i(t-2)} = \alpha_i\hat{x}_{i(t-2)} + (1-\alpha_i)\tilde{x}_{i(t-2)} \tag{10}$$

$$b_{i(t-2)} = \beta_i[S_{i(t-2)} - S_{i(t-3)}] + (1-\beta_i)b_{i(t-3)} \tag{11}$$

where α_i and β_i are constant parameters determined by trial and error. It is evident that the model parameters depend on previous states themselves. The above formulas were derived from the canonical representation of Holt's method [36].

In the DSE problem, $w_{i(t-1)}$ presents the small random fluctuation in the power system state. It is a function of the power system load, generation schedule, and network configuration associated with the corresponding time sample. The mean value of $w_{i(t-1)}$ is usually assumed to be zero; however, its variance is determined by either historical records of state variable changes or a series of off-line simulations.

B. State Estimation

SE (i.e., filtering) is the second stage of DSE that is executed upon receiving the measured data set. At this stage, both prediction and measurement sets are employed to reach to the best estimation of the power system state. Note that this feature is very desirable in WAMS in which the level of measurement redundancy is rather low since PMU devices are not deployed at all network buses [9].

Here, a new formulation of estimation process of DSE is presented. The estimation process is formulated based on the WLS model, which is widely used in the estimation problems. The objective function of the estimation stage is

$$\min\ J_t = \left\{ \sum_{i=1}^{\mathrm{NS}} \sum_{j=1}^{\mathrm{NM_i}} \frac{(\bar{x}_{ijt} - \hat{x}_{it})^2}{\bar{\sigma}^2_{ij}} + \sum_{i=1}^{\mathrm{NS}} \frac{(\tilde{x}_{it} - \hat{x}_{it})^2}{\tilde{\sigma}^2_{it}} \right\}. \tag{12}$$

The first term in (12) shows the weighted difference of the estimation with measurement and the second term represents the weighted difference between the estimation and prediction. In (12), the state variables are bus voltage phasor values processed in the polar coordinate (namely magnitude and phase angles). Note as well that PMU measurements are synchronized with respect to the time reference provided by GPS satellites, which eliminate the need for a reference bus angle as in conventional state estimators [37].

As discussed earlier, we should discard the predicted values from the estimation process in the drastic change condition. In this respect, two approaches are discussed as follows.

1) Discarding by Process: In this approach, the innovation process [30] is employed. Upon receiving the new WAMS data set, the predicted values are compared with new measurements, predictions which are far from the corresponding measurements are identified, and associated terms are omitted from (12). The remaining predictions along with all measurements establish the objective function (12). This optimization problem can readily be solved by calculating derivative of (12)

and equating it to zero. The solution would be

$$\hat{x}_{it} = \frac{\sum_{j=1}^{\mathrm{NM}_i} \frac{\bar{x}_{ijt}}{\bar{\sigma}_{ij}^2} + \frac{\tilde{x}_{it}}{\tilde{\sigma}_{it}^2}}{\sum_{j=1}^{\mathrm{NM}_i} \frac{1}{\bar{\sigma}_{ij}^2} + \frac{1}{\tilde{\sigma}_{it}^2}}, \quad i = 1, \ldots, N_s. \tag{13}$$

Using this approach, the solution of the optimization problem is readily computable and the time interval between estimations would be significantly decreased. There are, however, disadvantages attributed to this approach. The first issue is in relation with the comparison criteria. For each state variable, we might have several redundant measurements along with one prediction. It could be challenging to decide which one of the measurements should be considered to measure the distance of prediction. The other disadvantage of this approach is that when the prediction is compared with a measurement, or in general the equivalent of all measurements, the effect of prediction is not considered in the reference point. Whereas the inclusion of the impact of prediction in the comparison reference values would make the rejection process more authentic.

2) Simultaneous Discarding: Another technique is proposed here to overcome the disadvantages associated with the first approach. With the considerations discussed earlier, the second term of (12) should be omitted from the objective function during the sudden change condition. This characteristic is achievable by accommodating binary variables γ_{it} in (14)

$$\min J_t = \left\{ \sum_{i=1}^{\mathrm{NS}} \sum_{j=1}^{\mathrm{NM}_i} \frac{(\bar{x}_{ijt} - \hat{x}_{it})^2}{\bar{\sigma}_{ij}^2} + \sum_{i=1}^{\mathrm{NS}} (1 - \gamma_{it}) \frac{(\tilde{x}_{it} - \hat{x}_{it})^2}{\tilde{\sigma}_{it}^2} \right\}. \tag{14}$$

This binary variable is an indicator of the sudden change condition corresponding to the state variable i. One of the advance topics in SSE is the bad data identification and rejection. In [2], it has been pointed out that when the absolute value of the measurement residual is greater than the triple of the estimation standard deviation, there is a good chance that the corresponding measurement is bad. Comparing this subject with the prediction elimination reveals the same. Accordingly, the rule is employed to detect the sudden change condition. The prediction residual is represented by $\tilde{r}_{it}$ as

$$\tilde{r}_{it} = \left| \tilde{x}_{it} - \hat{x}_{it} \right|. \tag{15}$$

The following formulation is proposed for γ_{it}:

$$\frac{\tilde{r}_{it} - 3\hat{\sigma}_{it}}{M_i} \leq \gamma_{it} \leq \frac{\tilde{r}_{it} - 3\hat{\sigma}_{it}}{M_i} + 1 \tag{16}$$

where M_i is a positive constant number, which is always larger than the numerator. In (16), when $\tilde{r}_{it}$ is $<3\hat{\sigma}_{it}$, the lower limit of γ_{it} would be a small negative number and its upper limit would be a positive number smaller than unity. γ_{it} is consequently set to 0 and the prediction is included in objective function. Otherwise, for $\tilde{r}_{it} \geq 3\hat{\sigma}_{it}$, the variable γ_{it} is 1 and the prediction is excluded.

In (16), $\hat{\sigma}_{it}$ is the standard deviation associated with the estimation of variable i at time t; however, it is unknown as long as the estimated value of variable i is unknown. Accordingly, $\hat{\sigma}_{it}$ is a dependent variable, which is defined in terms of independent variables. Similar to the calculation of (13), the solution of (14) is given as

$$\hat{x}_{it} = \frac{\sum_{j=1}^{\mathrm{NM}_i} \frac{\bar{x}_{ijt}}{\bar{\sigma}_{ij}^2} + (1 - \gamma_{it}) \frac{\tilde{x}_{it}}{\tilde{\sigma}_{it}^2}}{\sum_{j=1}^{\mathrm{NM}_i} \frac{1}{\bar{\sigma}_{ij}^2} + (1 - \gamma_{it}) \frac{1}{\tilde{\sigma}_{it}^2}}. \tag{17}$$

If we apply the variance operator to (17) and assume that $\bar{x}_{ijt}$, $j = 1, 2, \cdots, N_m^i$, and $\tilde{x}_{it}$ are independent, we will have

$$\hat{\sigma}_{it} = \frac{1}{\sqrt{\sum_{j=1}^{\mathrm{NM}_i} \frac{1}{\bar{\sigma}_{ij}^2} + (1 - \gamma_{it}) \frac{1}{\tilde{\sigma}_{it}^2}}}. \tag{18}$$

The proposed model is summarized as follows: 1) (14) is the objective function; 2) (16) expresses the constraints; and 3) (15) and (18) define auxiliary variables. The solution methodology is proposed next.

The current representation of the model is highly nonlinear that includes the multiplication of a binary variable and a quadratic term in (14), absolute value function in (15), and binary variable in denominator in (18). Thus, the current model is the mixed-integer nonlinear program (MINLP). The present MINLP solvers are not powerful enough to effectively solve this type of problems even with a long execution time.

C. MIP-Based Formulation of SE

The efficient MIP solver can tackle very large-scale power system problems with thousands of continuous and integer variables within a tolerable time. It also guarantees a solution that is globally optimal or one that is within an acceptable tolerance. MIP proposes very flexible and accurate modeling capabilities which are extremely desirable in practical problems. MIP includes two types of problems: 1) mixed-integer linear programming (MILP) problems and 2) mixed-integer quadratic programming (MIQP) problems. MILP models comprise both linear objective function and constraints; while MIQP models consist of quadratic objective function but linear constraints. The latter is the case in this paper which is denoted as a MIP model hereafter. Substituting the residuals of measurement and prediction with $\bar{r}_{ijt}$ and $\tilde{r}_{it}$, respectively, and $(1 - \gamma_{it})(\tilde{r}_{it})^2$ with $(\tilde{R}_{it})^2$, the objective function (14) is rewritten as

$$\text{Min } J_t = \left\{ \sum_{i=1}^{\mathrm{NS}} \sum_{j=1}^{\mathrm{NM}_i} \frac{\bar{r}_{ijt}^2}{\bar{\sigma}_{ij}^2} + \sum_{i=1}^{\mathrm{NS}} \frac{\tilde{R}_{it}^2}{\tilde{\sigma}_{it}^2} \right\} \tag{19}$$

which is a quadratic function. To linearize $\tilde{R}_{it}$ in terms of γ_{it} and $\tilde{r}_{it}$, the following inequities are presented [38]:

$$r_i^{\min} (1 - \gamma_{it}) \leq \tilde{R}_{it} \leq r_i^{\max} (1 - \gamma_{it}) \tag{20}$$

$$\tilde{r}_{it} - r_i^{\max} \gamma_{it} \leq \tilde{R}_{it} \leq \tilde{r}_{it} - r_i^{\min} \gamma_{it}. \tag{21}$$

If $\hat{x}_{it}$ represents a voltage magnitude, $r_i^{\min}$ and $r_i^{\max}$ are selected as 0 and 2 (p.u.), respectively, and if $\hat{x}_{it}$ represents a voltage phase angle, $r_i^{\min}$ and $r_i^{\max}$ are set at $-\pi$ and

π (rad), respectively. When γ_{it} is equal to 1, $\tilde{R}_{it}$ will vanish due to (20) and the bounds in (21) will be inactive. Otherwise, when γ_{it} is equal to 0, (21) will enforce $\tilde{R}_{it}$ to be equal to $\tilde{r}_{it}$ and (20) will not bind $\tilde{R}_{it}$.

Here, (22)–(25) represent a set of linear expressions for $\bar{r}_{ijt}$ and $\tilde{r}_{it}$ in terms of $\hat{x}_{it}$

$$\bar{r}_{ijt} \geq \bar{x}_{ijt} - \hat{x}_{it} \tag{22}$$

$$\bar{r}_{ijt} \geq \hat{x}_{it} - \bar{x}_{ijt} \tag{23}$$

$$\tilde{r}_{it} \geq \tilde{x}_{it} - \hat{x}_{it} \tag{24}$$

$$\tilde{r}_{it} \geq \hat{x}_{it} - \tilde{x}_{it}. \tag{25}$$

Also, (18) is restated as a linear representation of $\hat{\sigma}_{it}$ in terms of γ_{it}

$$\hat{\sigma}_{it} = \frac{\gamma_{it}}{\sqrt{\sum_{j=1}^{\mathrm{NM}_i} \frac{1}{\bar{\sigma}_{ij}^2}}} + \frac{(1-\gamma_{it})}{\sqrt{\sum_{j=1}^{\mathrm{NM}_i} \frac{1}{\bar{\sigma}_{ij}^2} + \frac{1}{\tilde{\sigma}_{it}^2}}}. \tag{26}$$

Therefore, the SE problem is formulated in MIP. The estimated states $\hat{x}_{it}$ and its corresponding standard deviation $\hat{\sigma}_{it}$ will be calculated accordingly.

An important point is to be emphasized with regards to the detection/rejection of bad measurement data in estimators. WAMS is an accurate, reliable, viable, and secure measurement infrastructure. However, the inclusion of bad data detection/rejection in the proposed DSE, if intended, can be accommodated by adding a binary variable to the measurement residual term in (14).

The other issue is that the proposed model is on the basis that the state variables are the same as measurement quantities, which is the case in WAMS. This assumption does not hold in conventional metering system in which a nonlinear measurement function would correlate state variables with measurement quantities. Hence, the model proposed here is not applicable in a metering system composed of only conventional measurements. It should also be noted that due to inherent differences of conventional measurements with PMU data, which are being reported very fast and equipped with exact time stamps, adding conventional measurements to the WAMS is not a technically feasible choice. The reverse relation in which some PMU data are, however, being added to a SCADA system does make sense and is reported by several works. In such cases, the proposed DSE model could be used. To do so, an old-fashioned SE with only conventional measurements is first executed. Its output, which includes voltage magnitude and phase angle, is then considered as a set of phasor data for the proposed WAMS-based DSE [9].

V. Numerical Studies

In this section, a three-bus power system is analyzed to illustrate the performance of the proposed method. In addition, the effectiveness of the proposed method is examined on the IEEE 57-bus power system. Various scenarios are considered in each case for simulating sudden changes in the system state. The PMU locations are assumed to be given here. Additional PMU locations could be, however, examined for enhancing the performance of DSE.

Among performance indexes for quantifying the accuracy of state estimators, the root mean square deviation (RMSD) of estimated states is a commonly used indicator. Here, the RMSD of states corresponding to period t would be averaged over the entire time horizon

$$\mathrm{RMSD} = \frac{1}{\mathrm{NT}} \sum_{t=1}^{\mathrm{NT}} \sqrt{\frac{1}{\mathrm{NS}} \sum_{i=1}^{\mathrm{NS}} (\hat{x}_{it} - x_{it})^2}. \tag{27}$$

The above index is computed separately for voltage magnitudes and phase angles because these state variables have different scales. The estimator performance should be analyzed statistically for enhancing the reliability and generality of the obtained results. We consider 1000 executions with random measurement sets in which the performance indexes are averaged over all executions. The variability range (or standard deviation) of performance indexes is another index that would reflect the impact of measurement random errors on the overall performance of the estimator. The performance analysis is usually carried out considering various network topologies, loading levels, and generation dispatch. This requirement is satisfied in our analyzes since each execution has several time instants with a variety of scenarios.

In the following studies, true system states are represented by power flow solutions, measurements are simulated by adding random noises within designated ranges to true values, and prediction and estimated quantities are calculated based on the presentation in Section IV. Line parameter uncertainties are assumed to be typical as discussed in Section II, and PMU measurement errors are adopted based on the maximum allowable TVE (1%) associated with steady-state and small change conditions [24]. Since the drastic changes considered in this paper might correspond to dynamic conditions, the TVE associated with dynamic situations (3%) is also studied as part of sensitivity analyzes. In practical cases, appropriate and realistic values could be employed which depend on parameters specified by PMU manufacturers and experiences with periodical calibrations. The CPLEX solver in the general algebraic modeling system (GAMS) environment is employed for the optimization purpose and the simulations were carried out using an Intel Core (TM) i7 at 1.60-GHz CPU with 4 GB of RAM.

A. Three-Bus System

The three-bus power system is shown in Fig. 3 and the corresponding data are given in the Appendix (Tables VI and VII). The PMU located at bus 1 measures the voltage phasor of bus 1 and current phasors of transmission lines 1 and 2. Accordingly, the voltage phasors at buses 2 and 3 would be measured indirectly. According to the power flow solution, unit 1 would generate $0.8 + j\ 0.25$ (p.u. on the 100 MVA base) and the remaining load plus transmission system losses are generated by unit 2, which is located at the slack bus.

TABLE I
BINARY VARIABLES γ_{it} IN CASE 0

i	t																							
	1	2	3	4	5	6	7	8	9	10	11	12	13	14	15	16	17	18	19	20	21	22	23	24
V_1	0	0	0	0	0	0	0	1	1	1	1	1	1	1	0	1	1	0	0	1	1	0	1	1
δ_1	1	1	0	1	1	0	0	1	1	1	1	1	1	1	0	1	1	1	0	1	1	0	1	1
V_2	0	0	0	0	0	0	0	0	0	0	0	0	0	0	0	0	0	0	0	0	0	0	0	0
δ_2	1	1	0	0	0	0	0	1	0	0	0	0	0	0	0	0	0	0	0	0	0	0	0	1
V_3	0	0	0	0	0	0	0	0	1	1	1	0	0	0	0	0	0	0	0	1	1	0	1	1
δ_3	0	0	0	0	0	0	0	0	1	1	0	0	1	1	0	1	1	0	0	1	1	0	1	1

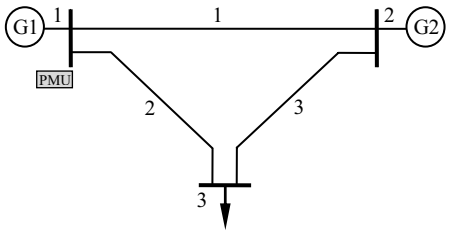

Fig. 3. Three-bus system.

The reference bus angle is not defined because of direct phase measurement of PMUs, and state variables are considered as $\{V_1, \delta_1, V_2, \delta_2, V_3, \delta_3\}$. The challenging situation for measuring the performance of DSE is a sudden change in system conditions. This condition is simulated via the following scenarios.

1) 20% load increase at time period 4.
2) Switch OFF generating unit 1 at time period 9.
3) Switch ON generating unit 1 at time period 13.
4) 20% load decrease at time period 16.
5) Switch out transmission line 3 at time period 20.
6) Switch in transmission line 3 at time period 23.

When unit 1 is on outage, the system load plus losses are fed by unit 2; thus, there would be no load curtailments. Note as well that the observability of the power system is preserved when transmission line 3 is on outage.

We consider the following three test cases.

Case 0: Base case including the simultaneous discarding capability.

Case 1: Exclude the discarding capability.

Case 2: Execute SSE with omitting the predictions.

These Cases are thoroughly discussed in the following.

Case 0: We have used the DSE formulation proposed in Section IV-C for 24 time periods. Although the performance of proposed DSE is generally drawn statistically, an execution of performance indexes around the average statistical values is adopted here for the sake of discussion. The binary variables γ_{it} are shown in Table I, in which 1 and 0 denote the discarding and inclusion of predictions, respectively. Not surprisingly, predictions associated with the state variables V_1 and δ_1 are discarded in most time instants. The reason is that V_1 and δ_1 have PMU direct measurements with higher accuracy as compared with indirect measurements at buses 2 and 3 where the uncertainty of transmission line parameters is considered. γ_{it} associated with V_2 is 0 as this state variable is regulated by unit 2 and would inherently remain fixed when volatile conditions are considered. γ_{it} associated with V_3 is 1 at time periods 9, 20, and 23, which correspond to scenarios 2), 5), and 6), respectively. In addition, $\gamma_{V_3,t}$ is 1 at instants 10, 11, 21, and 24, which is due to the memory of the prediction approach and large variations in the system operating conditions at the indicated scenarios. According to Table I, δ_3 is more sensitive to sudden change conditions as compared to other state variables, and its associated binary variables are 1 corresponding to all scenarios except 1).

Fig. 4 shows the DSE results in Case 0. The estimated bus voltage errors are computed for both magnitudes and phase angles as the difference between estimated and true values in the base case of power flow solutions. In Fig. 4, measurement errors are presented for state variables which are associated with PMU direct measurements at bus 1 and indirect measurements at buses 2 and 3. Time instants with lower estimation error demonstrate the impact of data redundancy in DSE. Time instants with identical estimation and measurement errors correspond to instants with prediction discarding, or $\gamma_{it} = 1$ in the mathematical sense. Fig. 4 shows that there is a similar error behavior for bus voltage magnitudes and phase angles in different buses. The reason is that only one PMU exists in the three-bus network and state variables at buses 2 and 3 are dependent on the PMU voltage measurement at bus 1.

Here, the binary variables associated with switching OFF and ON of generating unit 1 (or switching out and in of transmission line 3) are not necessarily the same although the scenarios have identical severities in terms of power systems. The reason is that the scenarios are not identical from the DSEs viewpoint as measurement errors are randomly different in various time instants. This observation would be less likely as we increase the redundancy levels of measurement systems. The data set would be prohibitively large if we present all state variables in the entire time horizon. Hence, Table II merely presents the measured, predicted, estimated, and true values of V_3, and δ_3 to provide a set of specific numerical representation for the DSE performance. These state variables would include 1 and 0 values for γ_{it} which can clarify the impact of prediction inclusion and rejection. In Table II, as expected, estimations are closer to the true state values as compared with the pure measurement data set. Since the measurement redundancy is zero in this case study, the analytical conclusions of the IEEE

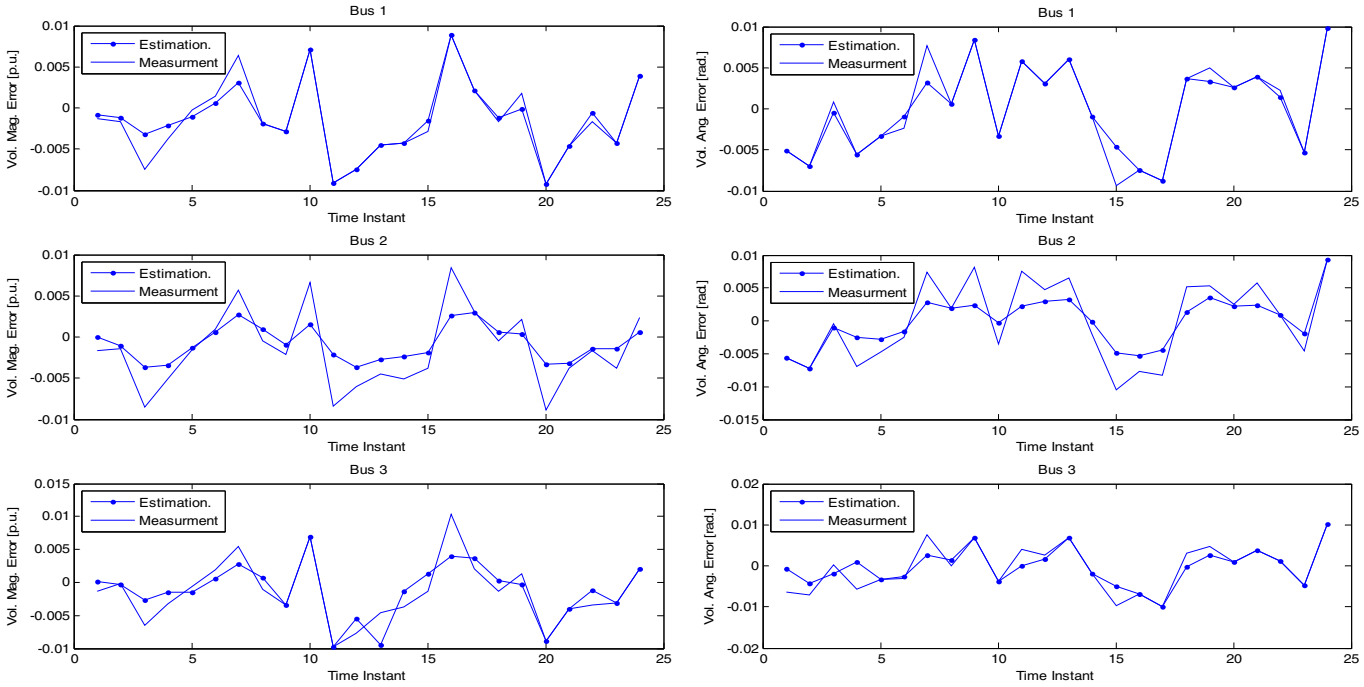

Fig. 4. Error in state variable estimation and measurement.

TABLE II
COMPARISON OF MEASUREMENT, PREDICTION, ESTIMATION, AND TRUE VALUES

t	Measurement		Prediction		Estimation		True		t	Measurement		Prediction		Estimation		True	
	V_3 (p.u.)	δ_3 (rad.)	V_3 (p.u.)	δ_3 (rad.)	V_3 (p.u.)	δ_3 (rad.)	V_3 (p.u.)	δ_3 (rad.)		V_3 (p.u.)	δ_3 (rad.)	V_3 (p.u.)	δ_3 (rad.)	V_3 (p.u.)	δ_3 (rad.)	V_3 (p.u.)	δ_3 (rad.)
1	0.996	-0.068	1.002	-0.047	0.997	-0.062	0.997	-0.061	13	0.984	-0.077	0.950	-0.128	0.980	-0.077	0.989	-0.083
2	0.996	-0.070	0.994	-0.077	0.996	-0.070	0.996	-0.063	14	0.986	-0.084	0.990	-0.021	0.988	-0.084	0.990	-0.082
3	0.989	-0.065	0.994	-0.081	0.993	-0.067	0.996	-0.065	15	0.989	-0.090	1.004	-0.092	0.992	-0.090	0.990	-0.080
4	0.984	-0.094	0.985	-0.066	0.985	-0.087	0.987	-0.088	16	1.010	-0.062	0.999	-0.096	1.003	-0.062	0.999	-0.055
5	0.988	-0.089	0.978	-0.103	0.987	-0.089	0.988	-0.086	17	1.001	-0.067	1.022	-0.033	1.002	-0.067	0.999	-0.057
6	0.990	-0.090	0.986	-0.099	0.988	-0.090	0.988	-0.087	18	0.997	-0.055	1.005	-0.072	0.999	-0.058	0.998	-0.058
7	0.992	-0.082	0.993	-0.092	0.992	-0.087	0.987	-0.090	19	1.000	-0.052	0.992	-0.050	0.998	-0.052	0.999	-0.057
8	0.986	-0.090	0.996	-0.077	0.987	-0.088	0.987	-0.090	20	0.939	-0.203	0.997	-0.045	0.939	-0.203	0.947	-0.204
9	0.956	-0.136	0.984	-0.089	0.956	-0.136	0.959	-0.143	21	0.938	-0.209	0.879	-0.355	0.938	-0.209	0.942	-0.213
10	0.967	-0.144	0.923	-0.185	0.967	-0.144	0.960	-0.140	22	0.933	-0.221	0.938	-0.215	0.935	-0.221	0.937	-0.222
11	0.952	-0.133	0.979	-0.153	0.952	-0.137	0.961	-0.137	23	0.993	-0.070	0.930	-0.230	0.993	-0.070	0.996	-0.065
12	0.954	-0.133	0.936	-0.129	0.954	-0.133	0.962	-0.136	24	0.997	-0.057	1.051	0.079	0.997	-0.057	0.995	-0.067

57-bus system are expected to be more general. The index defined in (27) considered for assessing the performance of the proposed DSE is calculated as $\text{RMSD}_m = 0.0038$ (p.u.) for voltage magnitudes and $\text{RMSD}_p = 0.0045$ (rad) for voltage phase angles. These indexes are calculated statistically with 1000 executions.

Case 1: In this case, the discarding capability is not considered and all predictions are included in the estimation process. Hence, the objective function (12) is considered with both measurement and prediction residuals, with a solution derived already in (13). This attribute shows that an optimization would not be required as the solution is obtained with a simple calculation. This simplicity is achieved at the cost of not omitting the drastic changes. The performance indexes associated with this case are $\text{RMSD}_m = 0.0046$ (p.u.) and $\text{RMSD}_p = 0.0056$ (rad).

Case 2: In this case, the state prediction is disregarded. By definition, this situation corresponds to the conventional SE, referred to as SSE. There is, however, only one measurement associated with each state variable and the SE leads to the measurement data set. Thus, the performance indexes of $\text{RMSD}_m = 0.0049$ (p.u.) and $\text{RMSD}_p = 0.0057$ (rad) are identical to the average values of RMSD of measurements. The comparison of performance indexes in Cases 1 and 2 with those in Case 0 verifies the advantage of using DSE for enhancing the estimation accuracy.

1) Sensitivity Analysis: Here, Case 3 is considered to extract the sensitivity of DSE performance in preserving or discarding the prediction terms with respect to measurement uncertainties. In this case, PMU measurement uncertainties are multiplied by three; thus, the confidence bounds of uncertain values are wider and equal to 3% which is the maximum allowable TVE of PMU measurements in dynamic conditions [24]. The measurements of V_2, δ_2, V_3, and δ_3 are more volatile and it is expected that the role of prediction would become more significant. Table III presents the binary variables in

TABLE III
BINARY VARIABLES γ_{it} IN CASE 3

i	t																							
	1	2	3	4	5	6	7	8	9	10	11	12	13	14	15	16	17	18	19	20	21	22	23	24
V_1	1	1	0	0	1	1	0	0	1	1	0	0	1	1	0	1	1	0	0	1	1	0	1	1
δ_1	0	0	0	1	1	0	0	0	1	1	0	1	1	1	0	0	0	0	0	1	1	1	1	1
V_2	0	0	0	0	0	0	0	0	0	0	0	0	0	0	0	0	0	0	0	1	1	0	0	0
δ_2	0	0	0	0	0	0	0	0	0	0	0	0	0	0	0	0	0	0	0	0	0	1	1	0
V_3	0	0	0	0	0	0	0	0	1	1	0	0	0	0	0	0	0	0	0	1	1	0	1	1
δ_3	0	0	0	0	0	0	0	0	1	1	0	0	1	1	0	0	0	0	0	1	1	0	1	1

which the predicted values associated with designated state variables are discarded. The performance indexes are $\text{RMSD}_m = 0.0160\,(\text{p.u.})$ and $\text{RMSD}_p = 0.0177$ (rad). This research is repeated when the predictions are not considered, namely SSE. The analysis results in performance indexes as $\text{RMSD}_m = 0.0271$ (p.u.) and $\text{RMSD}_p = 0.0306$ (rad). In this case, the relative improvements due to the inclusion of predictions in the estimation process are 40.5% and 42.1% for voltage magnitude and phase angle, respectively. The same comparison for the studies with 1% TVE in Cases 0 and 2 leads to 22.4% and 21.0% improvements for voltage magnitude and phase angle, respectively. Hence, predictions will have a higher positive impact on the estimation accuracy as we increase the measurement uncertainty.

B. IEEE 57-Bus System

The network topology is shown in Fig. 5 [39]. We disregard the zero-injection effect and use the PMU placement algorithm proposed in [25] which considers 17 PMUs at buses $\{1, 4, 6, 9, 15, 20, 24, 28, 30, 32, 36, 38, 41, 46, 50, 53, 57\}$ to make the system observable. The following scenarios would simulate conditions with sudden changes.

1) Load increase at buses 31–33 at time period 2.
2) Switch OFF generating unit 3 at time period 5.
3) Switch out transmission line 18–19 at time period 9.

We simulate 12 time periods with an active simultaneous discarding capability. Similar to the three bus example, buses with PMU experience more accurate measurements with their binary variables equal to 1 at most time periods. Hence, we hereafter focus on the binary variables of non-PMU buses. Among these variables, those which are equal to 1 are presented in Table IV. At time period 2, the loads at buses 31 to 33 are increased suddenly. The simulation results reveal that $\gamma_{V_b,t}$ associated with buses 25, 31, and 33 are equal to 1 at time periods 2 and 3. Similarly, $\gamma_{\delta_b,t}$ associated with buses 31, and 33 are equal to 1 at the same time periods. As expected, the buses experiencing sudden changes are geographically located in the vicinity of the one with the initial sudden change.

At time period 5, the generating unit 3 is switched OFF. The generation shortage is compensated for by unit 1 which shifts the state variables to a new operating point. The transition depends on the unit 5 dispatch which is 40 MW in this case. This event is not identified as a sudden change according to the binary variables associated with bus voltage magnitudes.

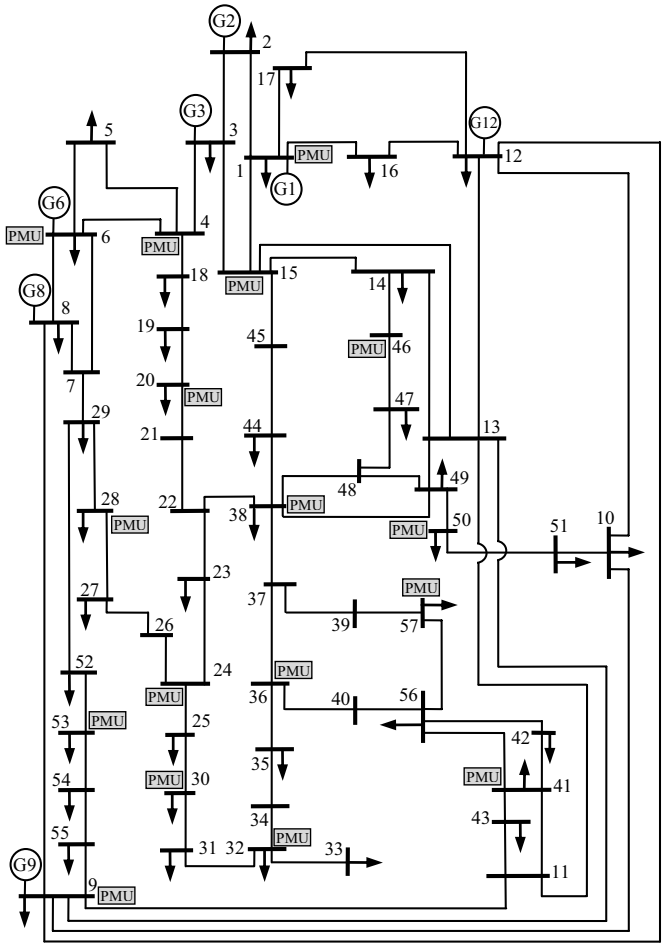

Fig. 5. One-line diagram of IEEE 57-bus system.

The observation is justified as the closely located generating units would prevent a significant voltage drop during the outage of generating unit 3. On the contrary, line flows and bus phase angles experience relatively large variations. Table IV shows that several binary variables associated with bus voltage angles would become 1 at time periods 5 and 6.

We switch out the transmission line 18–19 at time period 9. At time period 8, the active power flow from bus 18 to bus 19 is only 2 MW. Hence, the line outage would not impose a sever condition. Table IV shows that $\gamma_{V_b,t}$ and $\gamma_{\delta_b,t}$ associated with bus 19 is equal to 1 only at the instant of change occurrence. Hence, the impact of outage of line 18–19 is very limited.

TABLE IV
BINARY VARIABLES γ_{it} FOR THE IEEE 57-BUS POWER SYSTEM

t	Buses with $\gamma_{V_b,t}=1$	Buses with $\gamma_{\delta_b,t}=1$
2-3	25, 31, 33	31, 33
5-6	-	3, 5, 7, 14, 18, 19, 29
9	19	19

TABLE V
PERFORMANCE INDEXES AND EXECUTION TIMES FOR THE IEEE 57-BUS SYSTEM

Case	$RMSD_m$ (p.u.)	$RMSD_p$ (rad.)	Time (s)
0	0.0014	0.0012	1.56
1	0.0021	0.0023	0.83
2	0.0020	0.0023	0.68

We examine three case studies (Cases 0–2) of the three-bus system on the 57-bus test system. Similarly, 1000 simulations were carried out and the indexes were averaged. Table V shows the index (27) separately calculated for voltage magnitudes and phase angles. Here, the comparison of indexes with those of the three-bus system reveals that the utilization of prediction elimination capability would result in smaller improvements in system-wide indexes for larger systems. This observation is accurate since contingencies in larger systems would have limited geographically impacts with a smaller impact on the entire set of system state variables. Regarding the same RMSD_p in Cases 1 and 2, it is worth noting that the performance indexes are averaged over the entire time periods. For the time instants without drastic changes, the estimation errors in Case 1 are smaller. However, because the discarding capability is excluded, the predictions impose greater estimation errors for time periods associated with sudden changes. Furthermore, the predictions impose greater estimation errors for time periods associated with sudden changes because we exclude the discarding capability. This observation is critical as it reflects the necessity of accommodating discarding capability in the DSE.

Table V additionally presents a comparison of computation speed. As expected, Case 0 takes more time for optimization; however, the process would likely be faster than that of Case 1 when outlier predictions are eliminated iteratively. The other important point is that the execution time of Case 1 is not twice that of Case 2. This observation is sensible as the number of input data in Case 1 is not twice. In Case 2, 17 PMUs assigned to the IEEE 57-bus system offer many redundant indirect measurements; while, in Case 1, only 2×57 predictions are added to the input data set.

VI. CONCLUSION

The solution of DSE problem with the PMU measurements was addressed in this paper. The confidence level of measurements associated with buses without PMU was computed by propagating the uncertainties of original measurements over the transmission lines and considering a variation bound for the line parameters. The proposed MIP-based DSE formulation is equipped with simultaneous discarding capability of predictions. This feature alleviates the need for multiple executions of DSE for averting the performance degradation when predictions are included at periods with sudden changes. Two test systems were thoroughly examined and the effectiveness of the proposed model was verified by considering various conditions for loading and topology changes. As illustrated in this paper, the proposed formulation works effectively during both normal and sudden change conditions. At normal conditions, the prediction promotes the estimation accuracy and enhances the data redundancy. However, upon the occurrence of a major power system event, the predicted data set are discarded to preserve the estimation quality. The buses equipped with PMUs have more exact measurements in which the prediction does not play an important role. In contrast, buses without PMUs exploit the predicted data set throughout the normal condition and even during some small disturbances.

APPENDIX

A. Derivatives of GUM Application

The partial derivatives required for (3) and (4) are extracted in this section. Converting $V_r\angle\delta_r$ into the rectangular coordination, we get

$$V_r\angle\delta_r = V_r^R + jV_r^I \tag{A.1}$$

where $V_r = \sqrt{(V_r^R)^2 + (V_r^I)^2}$ and $\delta_r = \tan^{-1}(V_r^I/V_r^R)$.

Referring to (1), we can formulate V_r^R and V_r^I as follows:

$$V_r^R = V_s\cos(\varphi_1) - I_s Z\cos(\varphi_2) + V_s YZ\cos(\varphi_3) \tag{A.2}$$
$$V_r^I = V_s\sin(\varphi_1) - I_s Z\sin(\varphi_2) + V_s YZ\sin(\varphi_3). \tag{A.3}$$

Note that φ_1, φ_2, and φ_3 are defined after (1).

Partial derivatives of V_r and δ_r are expressed in terms of partial derivatives of V_r^R and V_r^I as follows:

$$\frac{\partial V_r}{\partial p} = \frac{V_r^R\frac{\partial V_r^R}{\partial p} + V_r^I\frac{\partial V_r^I}{\partial p}}{V_r}, \quad \forall p\in P \tag{A.4}$$
$$\frac{\partial \delta_r}{\partial p} = \frac{-V_r^I\frac{\partial V_r^R}{\partial p} + V_r^R\frac{\partial V_r^I}{\partial p}}{(V_r)^2}, \quad \forall p\in P \tag{A.5}$$

and partial derivatives of V_r^R and V_r^I are obtained as follows:

$$\frac{\partial V_r}{\partial V_s} = [(V_r^R\cos\varphi_1 + V_r^I\sin\varphi_1) + (V_r^R YZ\cos\varphi_3 + V_r^I YZ\sin\varphi_3)]/V_r \tag{A.6}$$
$$\frac{\partial V_r}{\partial \delta_s} = -V_s[(V_r^R\sin\varphi_1 - V_r^I\cos\varphi_1) + (V_r^R YZ\sin\varphi_3 - V_r^I YZ\cos\varphi_3)]/V_r \tag{A.7}$$
$$\frac{\partial V_r}{\partial I_s} = -Z(V_r^R\cos\varphi_2 + V_r^I\sin\varphi_2)/V_r \tag{A.8}$$
$$\frac{\partial V_r}{\partial \delta_{Is}} = I_s Z(V_r^R\sin\varphi_2 - V_r^I\cos\varphi_2)/V_r \tag{A.9}$$
$$\frac{\partial V_r}{\partial Z} = -[(V_r^R I_s\cos\varphi_2 + V_r^I I_s\sin\varphi_2) \tag{A.10}$$

$$- (V_r^R V_s Y \cos\varphi_3 + V_r^I V_s Y \sin\varphi_3)]/V_r$$

$$\frac{\partial V_r}{\partial \theta_z} = Z[(V_r^R I_s \sin\varphi_2 - V_r^I I_s \cos\varphi_2) \quad \text{(A.11)}$$
$$- (V_r^R V_s Y \sin\varphi_3 - V_r^I V_s Y \cos\varphi_3)/V_r$$

$$\frac{\partial V_r}{\partial Y} = V_s Z(V_r^R \cos\varphi_3 + V_r^I \sin\varphi_3)/V_r \quad \text{(A.12)}$$

$$\frac{\partial V_r}{\partial \theta_y} = -V_s Y Z(V_r^R \sin\varphi_3 - V_r^I \cos\varphi_3)/V_r \quad \text{(A.13)}$$

$$\frac{\partial \delta_r}{\partial V_s} = [(V_r^R \sin\varphi_1 - V_r^I \cos\varphi_1) \quad \text{(A.14)}$$
$$+ (V_r^R Y Z \sin\varphi_3 - V_r^I Y Z \cos\varphi_3)]/(V_r)^2$$

$$\frac{\partial \delta_r}{\partial \delta_s} = V_s[(V_r^R \cos\varphi_1 + V_r^I \sin\varphi_1) \quad \text{(A.15)}$$
$$+ (V_r^R Y Z \cos\varphi_3 + V_r^I Y Z \sin\varphi_3)]/(V_r)^2$$

$$\frac{\partial \delta_r}{\partial I_s} = -Z(V_r^R \sin\varphi_2 - V_r^I \cos\varphi_2)/(V_r)^2 \quad \text{(A.16)}$$

$$\frac{\partial \delta_r}{\partial \delta_{Is}} = -I_s Z(V_r^R \cos\varphi_2 + V_r^I \sin\varphi_2)/(V_r)^2 \quad \text{(A.17)}$$

$$\frac{\partial \delta_r}{\partial Z} = -[(V_r^R I_s \sin\varphi_2 - V_r^I I_s \cos\varphi_2) \quad \text{(A.18)}$$
$$- (V_r^R V_s Y \sin\varphi_3 - V_r^I V_s Y \cos\varphi_3)]/(V_r)^2$$

$$\frac{\partial \delta_r}{\partial \theta_z} = -Z[(V_r^R I_s \cos\varphi_2 + V_r^I I_s \sin\varphi_2) \quad \text{(A.19)}$$
$$- (V_r^R V_s Y \cos\varphi_3 + V_r^I V_s Y \sin\varphi_3)]/(V_r)^2$$

$$\frac{\partial \delta_r}{\partial Y} = V_s Z(V_r^R \sin\varphi_3 - V_r^I \cos\varphi_3)/(V_r)^2 \quad \text{(A.20)}$$

$$\frac{\partial \delta_r}{\partial \theta_y} = V_s Y Z(V_r^R \cos\varphi_3 + V_r^I \sin\varphi_3)/(V_r)^2. \quad \text{(A.21)}$$

The other parameters of (1) that should be calculated are σ_Z, σ_{θ_z}, $\sigma(Y)$, and $\sigma(\theta_y)$. Referring to Fig. 1, the polar representation of the line impedance and admittance are as follows:

$$Z = \sqrt{R^2 + X^2}, \quad \theta_z = \tan^{-1}(X/R) \quad \text{(A.22)}$$
$$Y = \sqrt{G^2 + B^2}, \quad \theta_y = \tan^{-1}(B/G). \quad \text{(A.23)}$$

Standard deviations of impedance and admittance amplitude and phase angle are function of line parameter variances, as given below

$$\sigma_Z = \sqrt{\left[\partial Z/\partial R\right]^2 [\sigma_R]^2 + \left[\partial Z/\partial X\right]^2 [\sigma_X]^2} \quad \text{(A.24)}$$
$$\sigma_{\theta_z} = \sqrt{\left[\partial \theta_z/\partial R\right]^2 [\sigma_R]^2 + \left[\partial \theta_z/\partial X\right]^2 [\sigma_X]^2} \quad \text{(A.25)}$$

where $\partial Z/\partial R = R/Z$,$\partial Z/\partial X = X/Z$,$\partial \theta_z/\partial R = -X/Z^2$, and $\partial \theta_z/\partial X = R/Z^2$.
And

$$\sigma_Y = \sqrt{\left[\partial Y/\partial G\right]^2 [\sigma_G]^2 + \left[\partial Y/\partial B\right]^2 [\sigma_B]^2} \quad \text{(A.26)}$$
$$\sigma_{\theta_y} = \sqrt{\left[\partial \theta_y/\partial G\right]^2 [\sigma_G]^2 + \left[\partial \theta_y/\partial B\right]^2 [\sigma_B]^2} \quad \text{(A.27)}$$

where $\partial Y/\partial G = G/Y$, $\partial Y/\partial B = B/Y$, $\partial \theta_y/\partial G = -B/Y^2$, and $\partial \theta_y/\partial B = G/Y^2$.

B. Three-Bus System Data

TABLE VI
TRANSMISSION LINE DATA

Line No.	From Bus	To Bus	R (p.u.)	X (p.u.)	G (p.u.)	B (p.u.)
1	1	2	0.05	0.2	0	0.025
2	1	3	0.02	0.15	0	0.02
3	2	3	0.02	0.15	0	0.02

TABLE VII
POWER SYSTEM LOAD IN 24 TIME PERIODS

t	P (p.u.)	Q (p.u.)	t	P (p.u.)	Q (p.u.)	t	P (p.u.)	Q (p.u.)
1	1.020	0.110	9	1.311	0.142	17	0.977	0.106
2	1.040	0.112	10	1.285	0.139	18	0.987	0.107
3	1.061	0.115	11	1.259	0.136	19	0.977	0.106
4	1.273	0.138	12	1.247	0.135	20	0.997	0.108
5	1.248	0.135	13	1.234	0.133	21	1.017	0.110
6	1.260	0.136	14	1.222	0.132	22	1.037	0.112
7	1.286	0.139	15	1.198	0.129	23	1.058	0.114
8	1.286	0.139	16	0.958	0.103	24	1.079	0.117

REFERENCES

[1] M. Shahidehpour, W. F. Tinney, and Y. Fu, "Impact of security on power systems operation," *Proc. IEEE*, vol. 93, no. 11, pp. 2013–2025, Nov. 2005.

[2] A. J. Wood and B. F. Wollenberg, *Power Generation, Operation, and Control*, 2nd ed. New York, NY, USA: Wiley, 1996.

[3] A. M. Leite da Silva, M. B. Do Coutto Filho, and J. M. C. Cantera, "An efficient dynamic state estimation algorithm including bad data processing," *IEEE Trans. Power Syst.*, vol. 2, no. 4, pp. 1050–1058, Nov. 1987.

[4] M. B. Do Coutto Filho and J. C. Stacchini de Souza, "Forecasting-aided state estimation—Part I: Panorama," *IEEE Trans. Power Syst.*, vol. 24, no. 4, pp. 1667–1677, Nov. 2009.

[5] M. B. Do Coutto Filho, J. C. S. de Souza, and R. S. Freund, "Forecasting-aided state estimation—Part II: Implementation," *IEEE Trans. Power Syst.*, vol. 24, no. 4, pp. 1678–1685, Nov. 2009.

[6] N. R. Shivakumar and A. Jain, "A review of power system dynamic state estimation techniques," in *Proc. IEEE Int. Conf. Power Syst. Technol.*, Oct. 2008, pp. 1–6.

[7] A. Jain and N. R. Shivakumar, "Power system tracking and dynamic state estimation," in *Proc. Power Syst. Conf. Expos.*, Mar. 2009, pp. 1–8.

[8] A. G. Phadke and R. M. de Moraes, "The wide world of wide-area measurement," *IEEE Power Energy*, vol. 6, no. 5, pp. 52–65, Oct. 2008.

[9] G. Phadke and J. S. Thorp, *Synchronized Phasor Measurements and Their Applications*. New York, NY, USA: Springer-Verlag, 2008.

[10] A. Jain and N. R. Shivakumar, "Impact of PMUs in dynamic state estimation of power systems," in *Proc. 40th NAPS*, Sep. 2008, pp. 1–8.

[11] H. Xua, Q. Jia, N. Wang, Z. Bo, H. Wang, and H. Ma, "A dynamic state estimation method with PMU and SCADA measurement for power systems," in *Proc. IPEC*, Dec. 2007, pp. 848–853.

[12] N. R. Shivakumar and A. Jain, "Including phasor measurements in dynamic state estimation of power systems," in *Proc. Int. Conf. Power Syst. ACO*, Mar. 2008, pp. 1–6.

[13] E. Farantatos, G. K. Stefopoulos, G. J. Cokkinides, and A. P. Meliopoulos, "PMU-based dynamic state estimation for electric power systems," in *Proc. Power Energy Soc. General Meeting*, Jul. 2009, pp. 1–8.

[14] A. Jain and N. R. Shivakumar, "Phasor measurements in dynamic state estimation of power systems," in *Proc. IEEE Region 10th Conf. TENCON*, Nov. 2008, pp. 1–6.

[15] Z. Huang, K. Schneider, and J. Nieplocha, "Feasibility studies of applying Kalman Filter techniques to power system dynamic state estimation," in *Proc. Int. Power Eng. Conf.*, Dec. 2007, pp. 376–382.

[16] EPRI. (2008). *Next Generation State Estimation (Predictive, Dynamic With System Identification)*, Charlotte, NC, USA [Online]. Available: http://portfolio.epri.com/

[17] S. Chakrabarti and E. Kyriakides, "PMU measurement uncertainty considerations in WLS state estimation," *IEEE Trans. Power Syst.*, vol. 24, no. 2, pp. 1062–1071, May 2009.

[18] A. Abur and A. G. Expósito, *Power System State Estimation: Theory and Implementation*. New York, NY, USA: Marcel Dekker, 2004.

[19] (2013). *High-Performance Mathematical Programming Solver for Linear Programming, Mixed Integer Programming, and Quadratic Programming* [Online]. Available: http://www.ilog.com/products/cplex/

[20] S. Chakrabarti, E. Kyriakides, and M. Albu, "Uncertainty in power system state variables obtained through synchronized measurements," *IEEE Trans. Instr. Meas.*, vol. 58, no. 8, pp. 2452–2458, Aug. 2009.

[21] J. K. Al-Othman and M. R. Irving, "Analysis of confidence bounds in power system state estimation with uncertainty in both measurements and parameters," *Elec. Power Syst. Res.*, vol. 76, no. 12, pp. 1011–1018, Aug. 2006.

[22] J. Zhu, A. Abur, M. J. Rice, G. T. Heydt, and S. Meliopoulos, "Enhanced state estimators," PSERC, Tempe, AZ, USA, Tech. Rep. 06-45, Nov. 2006.

[23] *Performance Requirements Part II Targeted Applications: State Estimation*, PRTT, New York, NY, USA, Nov. 2005.

[24] *IEEE Standard for Synchrophasor Measurements for Power Systems*, IEEE Standard C37.118.1-2011, Dec. 2011.

[25] F. Aminifar, A. Khodaei, M. Fotuhi-Firuzabad, and M. Shahidehpour, "Contingency-constrained PMU placement in power networks," *IEEE Trans. Power Syst.*, vol. 25, no. 1, pp. 516–523, Feb. 2010.

[26] F. Aminifar, M. Fotuhi-Firuzabad, and A. Safdarian, "Optimal PMU placement based on probabilistic cost/benefit analysis," *IEEE Trans. Power Syst.*, vol. 28, no. 1, pp. 566–567, Feb. 2013.

[27] F. Aminifar, M. Fotuhi-Firuzabad, M. Shahidehpour, and A. Safdarian, "Impact of WAMS malfunction on power system reliability assessment," *IEEE Trans. Smart Grid*, vol. 3, no. 3, pp. 1302–1309, Sep. 2012.

[28] F. Aminifar, M. Fotuhi-Firuzabad, M. Shahidehpour, and A. Khodaei, "Observability enhancement by optimal PMU placement considering random power system outages," *Energy Syst.*, vol. 2, no. 1, pp. 45–65, Mar. 2011.

[29] M. B. D. C. Filho, A. M. L. da Silva, J. M. C. Cantera, and R. A. da Silva, "Information debugging for real-time power systems monitoring," *IEE Proc. Generat. Trans. Distribut.*, vol. 136, no. 3, pp. 145–152, May 1989.

[30] K. Nishiya, J. Hasegawa, and T. Koike, "Dynamic state estimation including anomaly detection and identification for power systems," *IEE Proc. Generat. Trans. Distribut.*, vol. 129, no. 5, pp. 192–198, Sep. 1982.

[31] A. M. Leite da Silva, M. B. Do Coutto Filho, and J. F. de Queiroz, "State forecasting in electric power systems," *IEE Proc. Generat. Trans. Distribut.*, vol. 130, no. 5, pp. 237–244, Sep. 1983.

[32] J. K. Mandal, A. K. Sinha, and L. Roy, "Incorporating nonlinearities of measurement function in power system dynamic state estimation," *IEE Proc. Generat Trans. Distribut.*, vol. 142, no. 3, pp. 289–296, May 1995.

[33] K. R. Shih and S. J. Huang, "Application of a robust algorithm for dynamic state estimation of a power system," *IEEE Trans. Power Syst.*, vol. 17, no. 1, pp. 141–147, Feb. 2002.

[34] S. J. Huang and K. R. Shih, "Dynamic-state-estimation scheme including nonlinear measurement-function considerations," *IEE Proc. Generat. Trans. Distribut.*, vol. 149, no. 6, pp. 673–678, Nov. 2002.

[35] J. M. Lin, S. J. Huang, and K. R. Shih, "Application of sliding surface-enhanced control for dynamic state estimation of a power system," *IEEE Trans. Power Syst.*, vol. 18, no. 2, pp. 570–577, May 2003.

[36] S. G. Makridakis, S. C. Wheelwright, and V. E. McGee, *Forecasting: Methods and Applications*. New York, NY, USA: Wiley, 1983.

[37] J. Zhu and A. Abur, "Effect of phasor measurements on the choice of references bus for state estimation," in *Proc. IEEE Power Eng. Soc. General Meeting*, Jun. 2007, pp. 1–5.

[38] C. A. Floudas, *Nonlinear and Mixed-Integer Optimization: Fundamentals and Applications*. New York, NY, USA: Oxford Univ. Press, 1995.

[39] (2013). *MATPOWER: A MATLAB Power System Simulation Package* [Online]. Available: http://www.pserc.cornell.edu/matpower

Farrokh Aminifar (S'07–M'11) received the B.Sc. (Hons.) degree from the Iran University of Science and Technology, Tehran, Iran, in 2005, and the M.Sc. (Hons.) and Ph.D. degrees from the Sharif University of Technology, Tehran, in 2007 and 2010, respectively, all in electrical engineering.

He has been collaborating with the Robert W. Galvin Center for Electricity Innovation with the Illinois Institute of Technology, Chicago, IL, USA, since March 2009. He is currently an Assistant Professor with the School of Electrical and Computer Engineering, the University of Tehran, Tehran. His research interests include wide-area measurement systems, reliability modeling and assessment, and smart grid technologies.

Dr. Aminifar has served as the Guest Editor of two Special Issues (Microgrids and Smart DC Distribution Systems) of the IEEE TRANSACTIONS ON SMART GRID. He received the IEEE Best Ph.D. Dissertation Award from the Iran Section for his research on the probabilistic schemes for the placement of pharos measurement units.

Mohammad Shahidehpour (F'01) is the Bodine Chair Professor and Director of the Robert W. Galvin Center for Electricity Innovation with the Illinois Institute of Technology, Chicago, IL, USA. He is a Research Professor with King Abdulaziz University, Jeddah, Saudi Arabia, North China Electric Power University, Beijing, China, and the Sharif University, Tehran, Iran. He was the general chair of the 2012 IEEE Innovative Smart Grid Technologies Conference, and Chair of the 2012 Great Lakes Symposium on Smart Grid and the New Energy Economy. He is the Editor-in-Chief of the IEEE TRANSACTIONS ON SMART GRID and an IEEE Distinguished Lecturer. He is a recipient of the 2012 IEEE PES Outstanding Power Engineering Educator Award. He was a recipient of the 2009 Honorary Doctorate from the Polytechnic University of Bucharest, Romania.

Mahmud Fotuhi-Firuzabad (SM'99) received the B.S. and M.S. degrees in electrical engineering from Sharif University of Technology, Tehran, Iran, and Tehran University, Tehran, in 1986 and 1989, respectively, and the M.S. and Ph.D. degrees in electrical engineering from the University of Saskatchewan, Saskatoon, SK, Canada, in 1993 and 1997, respectively.

He joined the Department of Electrical Engineering, the Sharif University of Technology, in 2002. Currently, he is a Professor and the Head of the Department of Electrical Engineering, Sharif University of Technology. He is an Honorary Professor with the Universiti Teknologi Mara, Shah Alam, Malaysia.

Dr. Fotuhi-Firuzabad is a member of the Center of Excellence in Power System Management and Control. He serves as an Editor of the IEEE TRANSACTIONS ON SMART GRID.

Saeed Kamalinia (S'07–M'11) received the B.S. and M.S. degrees in electrical engineering from the University of Tehran, Tehran, Iran, in 2005 and 2007, respectively, and the Ph.D. degree in electrical engineering from the Illinois Institute of Technology, Chicago, IL, USA, in 2010. He is currently a Project Engineer with S&C Electric Company-Power System Solutions, Chicago. His research interests include operation and control of power systems and integration of renewable energy resources.

Dr. Kamalinia is the Chair of Award Committee at IEEE-Chicago Section and a member of two technical working groups in Cigré.